Thermal vacancies in solid ^{3}He

S. M. Heald,* D. R. Baer,† and R. O. Simmons
Department of Physics and Materials Research Laboratory, University of Illinois at Urbana-Champaign, Urbana, Illinois 61801
(Received 16 April 1984)

Thermal vacancy concentrations in crystals of ^{3}He have been directly determined from measurements of the temperature dependence of the x-ray lattice parameter. Body-centered-cubic ^{3}He was studied for molar volumes ranging from 20.3 to 24.8 cm^3/mole for which the melting temperatures range from 2.36 to 0.435 K, respectively. It was found to contain about 0.5% thermal vacancies at melting, essentially independent of molar volume. A single hcp ^{3}He crystal (18.8 cm^3/mole) was studied, and was found to have 0.1% thermal vacancies at melting. From the measured vacancy concentrations, free energies of formation are obtained and compared with results from NMR and ultrasonic experiments. These comparisons suggest that in the bcc phase vacancies move by a tunneling process, while in the hcp phase their motion is thermally activated. Free volumes of formation are found from a comparison of the measured vacancy concentrations with existing thermal expansion and compressibility measurements. In the bcc phase the formation free volume is found to vary from $0.4v_a$ at 20 cm^3/mole to $0.3v_a$ at 24 cm^3/mole, where v_a is an atomic volume. The apparent heat capacity of the vacancies is calculated with use of a localized vacancy model and found to be unreasonably high. Both this result and an analysis of the volume of formation suggest that the vacancies are nonlocalized.

I. INTRODUCTION

Solid helium is a very interesting system in which to study thermal vacancies. Its large compressibility means that vacancies can be studied over a wide range of molar volumes using easily attainable pressures. Thus the volume dependence of the various parameters describing the vacancies can be determined. Helium also exists in two structures at rather modest pressures. At low pressures ^{3}He is in the body-centered-cubic (bcc) structure, which is loosely packed and allows the atoms a relatively large freedom of motion away from their equilibrium positions. At higher pressure solid ^{3}He forms in the hexagonal close packed (hcp) structure. The influence of crystal structure on vacancy formation and motion can hence be studied.

Also peculiar to solid helium is the dominance of quantum effects due to the large zero-point motion of the atoms. This affects the study of vacancies in two ways. First, each vacancy may not be localized on one lattice site. This idea has been discussed theoretically by several authors,[1–8] who all agree that nonlocalized vacancies or "vacancy waves" should exist with a band of excitation energies. This could result in a deviation of the vacancy concentration from classical Arrhenius behavior. However, experimental evidence for nonlocalized vacancies is still inconclusive. The second result of the quantum nature of helium is that vacancies can make a significant contribution to the thermal properties of the solid. The large zero-point motion of the atom means that solid helium melts at temperatures $T \lesssim 0.1\Theta_D$ where Θ_D is the equivalent Debye temperature. Therefore, the thermal vibrational contributions to the properties at melting do not overshadow the vacancy contribution as is the case for almost all other solids.

Most previous information about vacancies in solid ^{3}He has come from indirect sources. Nuclear magnetic resonance (NMR) experiments[8–11] are sensitive to the vacancy concentration as a result of the atomic motion which occurs as the vacancies change atomic sites. Another source of indirect information is precise measurements of ultrasonic velocity and attenuation changes.[12,13] It is possible to introduce dislocation pinning in helium at low temperatures and to follow depinning by a thermally activated process, as a solid specimen is heated to successively higher temperatures. These techniques depend upon diffusive properties of the defects and not the actual formation properties. In fact, from such measurements alone, one cannot be sure that the observed diffusion is due to vacancies instead of some other mechanism. However, once the nature of the diffusive mechanism is established, NMR and ultrasonic experiments have the advantage of high sensitivity.

Other indirect inferences about thermally-generated defects have come from heat-capacity measurements.[14–17] These depend, however, upon additional assumptions, such as the form of the defects, the photon contributions to the heat capacity, and other possible excitations. Such indirect inferences must be treated with great caution. The specific heat in the absence of vacancies has not been independently measured.

A more direct method of measuring vacancy concentrations is by x-ray diffraction techniques. Thermal vacancy concentration C can be found by using the relation

$$C=\frac{n}{N+n+n_z}=3\left[\frac{\Delta l}{l_0}-\frac{\Delta a}{a_0}\right] \tag{1}$$

for a cubic crystal. N is the number of atoms, n is the number of thermal vacancies, and n_z is the number of hy-

pothetical zero-point vacancies. l is a macroscopic length, a is the x-ray lattice parameter, and the subscript 0 refers to values in the absence of thermal vacancies. Thus Eq. (1) states that the thermal vacancy concentration is equal to the change in macroscopic volume minus the change in the microscopic x-ray volume. Since n_z is at most a few percent of N, for the most cases it can be ignored in the application of Eq. (1). Also, for helium constant macroscopic volume conditions can be closely achieved which means Eq. (1) becomes

$$C=\frac{n}{N+n+n_z}=-3\frac{\Delta a}{a_0}\ . \tag{2}$$

The validity of Eq. (1) has been considered in several articles,[18–20] and successful applications to the heavier noble-gas solids has been made.[21–24] Equation (1) [or equivalently Eq. (2)] has not been rigorously shown to apply to the case of nonlocalized vacancies. However, since a nonlocalized vacancy state can be written as a linear combination of localized vacancy states, it seems reasonable to assume that Eq. (1) applies equally well to helium. This assumption is made throughout the rest of this paper.

Partial experimental justification for the application of Eq. (2) to bcc ^{3}He is obtained from the pioneering work of Balzer and Simmons.[25] Although their measurements were limited in scope, they found a reversible change in the lattice parameter, and showed that the thermal defects observed in NMR measurements are indeed vacancies as predicted by theory.

The present work[26] greatly extends the measurements of Balzer and Simmons on ^{3}He to cover much wider ranges of molar volume and temperature. Extension of the measurements to small molar volumes (high pressures) allows the first direct observation of vacancies in the hcp ^{3}He phase to be made. The extension of the measurements to lower temperatures means that a reference state almost devoid of thermal vacancies can be achieved. Thus, for the first time knowledge of the absolute number of thermal vacancies is obtained. Consequently, such vacancy parameters as the free energy of formation and the free volume of formation can be calculated. It is also possible to commence detailed comparisons of various measurements to check for consistency with localized and nonlocalized vacancy models.

II. THEORY

A. Thermodynamics

Most previous work[27] on the thermodynamics of vacancy formation is concerned with the constant-pressure situation where the total Gibb's free energy must be minimized. For the constant-volume case only the Helmholtz free energy $F(V,T)$ need be minimized.[28] Following analogous arguments as for the constant-pressure case, we obtain for the concentration of noninteracting vacancies

$$C=e^{-f_v/kT}\ , \tag{3}$$

where

$$f_v=e_v-Ts_v \tag{4}$$

is the vacancy free energy of formation and the subscript v indicates the parameters referring to a vacancy formed at constant volume. e_v and s_v are the energy and nonconfigurational entropy of formation, respectively, which obey the following thermodynamic relations:

$$e_v=-T^2\left[\frac{\partial(f_v/T)}{\partial T}\right]_V\ , \tag{5}$$

and

$$s_v=-\left[\frac{\partial f_v}{\partial T}\right]_V\ . \tag{6}$$

For later use we also write the pressure of formation on the vacancy. The pressure of formation at constant volume is the analog of the volume of formation at constant pressure and is related to f_v by

$$p_v=-\left[\frac{\partial f_v}{\partial V}\right]_T\ . \tag{7}$$

Because the constant-pressure situation is more common than the constant-volume situation, calculations of vacancy properties have generally been done for the constant-pressure case. Since most experiments on helium are done at constant volume it is useful to have relations between corresponding isobaric and isochoric parameters.

We start with the observation that for a given pressure, volume, and temperature the number of vacancies is independent of how the state was achieved. Therefore, we have

$$g_p(T)=f_v(T)\ , \tag{8}$$

where g_p is the Gibbs free energy of formation at constant pressure. When a vacancy is created at constant volume the pressure will rise an amount dP. Equation (8) then becomes

$$f_v(T+dT)=g_{p+dp}(T+dT)=g_p(T+dT)+v_p dP\ , \tag{9}$$

where $v_p=\partial g_p/\partial P$ is the isobaric free volume of formation. Using Eqs. (5) and (6),

$$e_v=h_p-v_pT\left[\frac{\partial P}{\partial T}\right]_V\ , \tag{10}$$

$$s_v=s_p-v_p\left[\frac{\partial P}{\partial T}\right]_V\ , \tag{11}$$

where $h_p=e_p+Pv_p$ is the isobaric enthalpy of formation. By applying the same arguments to the constant-pressure situation it can be shown that

$$p_v=\frac{v_p}{v_a}B_T \tag{12}$$

where B_T is the isothermal bulk modulus and v_a is the atomic volume.

B. Vacancy contribution to crystal properties

The vacancy contribution to the properties of a crystal has been thoroughly discussed by several authors[27,29] for the isobaric case. Reference 28 is a detailed discussion for constant volume. This section gives some of the relevant results for later reference.

With the assumption of noninteracting monovacancies the free energy of the entire crystal can be written

$$F=F_0+nf_v-Ts_c \ . \tag{13}$$

F_0 is the free energy in the absence of vacancies and s_c is a configurational entropy term. With Eq. (13) the energy of the crystal is

$$E=E_0+ne_v \tag{14}$$

which gives the vacancy contribution to the constant-volume heat capacity as

$$C_V-C_V^0=n\left[\frac{\partial e_v}{\partial T}\right]_V+e_v\left[\frac{\partial n}{\partial T}\right]_V . \tag{15}$$

For localized vacancies $n\simeq N\exp(-f_v/kT)$ and we have

$$C_V-C_V^0\simeq n\left[\left[\frac{\partial e_v}{\partial T}\right]_V+\frac{e_v^2}{kT^2}\right] . \tag{16}$$

Similar relations can be derived for other properties of a solid and these are listed in Table I. It is straightforward to extend these relations to include the effects of divacancies and larger vacancy clusters, although the expressions themselves rapidly become very complicated.

For example, the equilibrium concentration of the jth type of vacancy cluster is given by a generalization of Eq. (3),

$$C_j=\frac{n_j}{N+n_n}=K_j e^{s_v^j/k}e^{-e_v^j/kT} , \tag{17}$$

where K_j is a geometrical factor related to the number of ways of orienting the defect in the lattice. For localized monovacancies, $K_1=1$, and for localized divacancies in a bcc lattice $K_2=4$. The free energy of formation for the jth type defect can be written as

$$f_v^j=jf_v-b_j \ , \tag{18}$$

where b_j is the binding free energy associated with the formation of the cluster from j monovacancies. Because of the binding free energy such parameters as the energy of formation and volume of formation will be different from the values associated with j monovacancies. In practice we expect that only the case of $b_j>0$ has to be considered, which means the energy and volume will be reduced from their corresponding monovacancy values. Considering only vacancies and divacancies, and using Eq. (17), it is thus easy to generalize Eq. (16),

$$C_V-C_V^0\simeq n_1\left[\left[\frac{\partial e_v}{\partial T}\right]_V+\frac{(e_v)^2}{kT^2}\right]+n_2\left[\left[\frac{\partial e_v^2}{\partial T}\right]_V+\frac{(e_v^2)^2}{kT^2}\right] . \tag{19}$$

Self-diffusion is another process in which vacancies may participate.[8] At temperatures near melting, diffusion and ionic conductivity acquire the Arrhenius behavior characteristic of a thermally activated process, at least for ^{3}He molar volumes less than 24 cm^3.

Nuclear magnetic resonance experiments measure the diffusion of ^{3}He atoms which at high temperatures move through the lattice with a characteristic frequency, $\omega_3=C\omega_d$. Here C is the vacancy concentration and ω_d is a characteristic frequency for vacancy motion. The temperature dependence of ω_d depends on the process by which the vacancies move. If they move by classical diffusion then a ^{3}He atom must jump over a potential barrier to reach the vacant site. ω_d is then thermally activated

TABLE I. Noninteracting monovacancy contribution to the properties of a solid. The symbols are n—number of vacancies, h_p—isobaric formation enthalpy, v_a—atomic volume, v_p—vacancy volume, V—crystal volume, p_v—isochoric pressure of formation. The superscript 0 signifies the property in the absence of vacancies. These formulas are compiled from Refs. 27–29.

Property	Vacancy contribution
Isobaric heat capacity	$C_p-C_p^0=n\left[\left[\frac{\partial h_p}{\partial T}\right]_p+\frac{h_p^2}{KT^2}\right]$
Thermal expansion	$\alpha-\alpha^0=\frac{n}{Nv_a}\left[\left[\frac{\partial v_p}{\partial T}\right]_p+\frac{v_p}{T}\frac{h_p}{KT}\right]$
Isothermal compressibility	$\beta_T-\beta_T^0=\frac{n}{Nv_a}-\left[\left[\frac{\partial v_p}{\partial P}\right]_T+\frac{v_p^2}{kT}\right]$
Pressure	$P-P^0=np_v$
Bulk modulus	$B_T-B_T^0=nNv_a\left[\left[\frac{\partial p_v}{\partial V}\right]_T+\frac{p_v^2}{kT}\right]$

and ω_3 has an associated diffusion activation energy $e_d = E_b + e_v$ where E_b is the barrier height. There may also be an entropy of migration associated with jumping over the barrier, but this is incorporated into the preexponential factor. If the vacancies tunnel then it is shown in Ref. 30 that for a bcc lattice $\omega_d = 5.2\omega_v$, where ω_v is the rate at which a ^{3}He atom tunnels into an adjacent vacant site. This results in ω_d being temperature independent and gives $e_d = e_v$.

III. EXPERIMENTAL PROCEDURE

A. Apparatus

The cryostat[31] and x-ray diffractometer[32] used for this work have been described elsewhere. Figure 1 shows a schematic drawing of the arrangement of the cryostat and x-ray diffractometer. The specimen crystal is held in fixed orientation and location in space, and the diffractometer is used to scan the x-ray tube and photon detector slit about it. The scanning, in opposite angular directions, can be succinctly described as Θ-Θ scans of the source and detector, respectively.

The system was controlled by a Digital Equipment Corporation PDP-8/L interfaced to the external equipment through the "Blox" system developed at the University of Illinois. A standard NaI scintillation detector and ancilliary electronic components were used. The scans were semiautomatic with the scan being halted at its midpoint to allow the reading of a dial indicator at a reference angle. A representative Cu $K\alpha$ (110) peak step scan in shown in Fig. 2. Note that the total background (from specimen pressure cell, cryostat radiation, and vacuum shields) is relatively low. When a scan was completed the diffractometer was automatically readied for a new scan. The system rapidly measures changes in lattice parameter, even from weakly scattering He crystals, but it cannot determine lattice parameters absolutely.

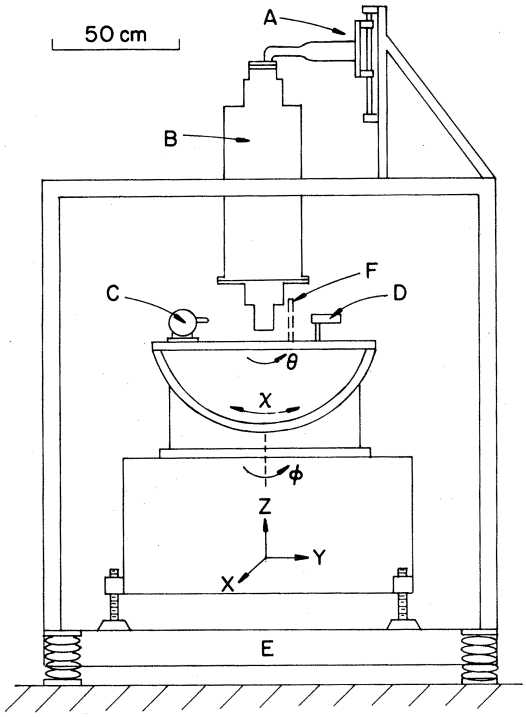

FIG. 1. Relative arrangement of the special three-circle x-ray diffractometer, the cryostat (Ref. 31) and the cryostat support frame. A, movable pumping-line support; B, cryostat; C, commercial x-ray tube with pinhole collimator; D, detector; E, concrete inertia block. After a helium crystal is grown, it is examined and its orientation determined using a Laue transmission cassette, F. With cassette removed, the detector is used as X and Y translations center the cell; Z motion selects the height. The angles ϕ and χ are then manually set and the Θ-Θ mechanism initialized for scanning a Bragg peak to measure lattice parameter changes.

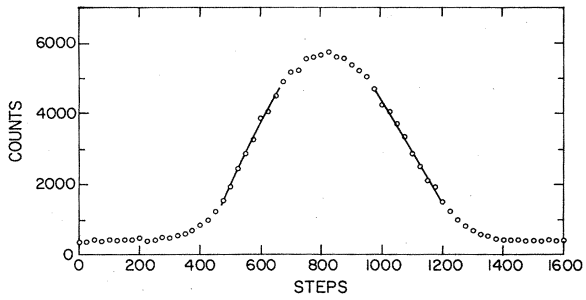

FIG. 2. Bragg-peak Θ-Θ scan, 6 sec/step. The solid lines are quadratic least-squares fits used for finding the peak location by bisection of chords drawn between them. Reproducibility of finding the location on repeated scans was 2 to 3 steps, which is equivalent to about 50 ppm relative change in ^{3}He lattice parameter.

B. Thermometry

A germanium resistance thermometer provided the primary temperature indication above 200 mK. Below 200 mK a Speer $\frac{1}{2}$-W, 100-Ω carbon resistor was used. Comparison of the germanium and Speer resistors above 200 mK provided the small correction ($\lesssim 3\%$) which necessarily had to be applied to the Speer calibration after each thermal cycling to room temperature. Both resistors were initially calibrated in a separate cryostat against the ^{3}He vapor pressure scale above 1 K, and against a cerium magnesium nitrate (CMN) magnetic thermometer below 1 K. The CMN thermometer itself was calibrated against the ^{3}He vapor-pressure scale above 1 K. In addition, the calibrations were checked with a National Bureau of Standards (NBS) superconducting fixed-point thermometer at 0.840, 1.172, and 3.414 K. The absolute accuracy of the calibration is estimated to be about 0.5% over the range from 0.06 to 3.40 K.

A second germanium thermometer was located at the bottom of the sample cell in order to monitor the temperature gradients across the cell (the top of the cell was fastened to the mixing chamber of a ^{3}He-^{4}He dilution refrigerator on which the other calibrated thermometers were also attached). This gradient thermometer was calibrated in place against the top thermometers. This was done twice, once with liquid in the cell and once with

solid in the cell. No difference was found indicating negligible gradients across the cell, since the solid is an order of magnitude better thermal conductor than the liquid. Also, the calibration of the bottom thermometer was repeatedly checked against the melting pressure of ^{3}He. No discrepancies were ever found.

C. Sample preparation

The crystals were grown from ^{3}He with a ^{4}He impurity of less than 300 ppm by cooling the top of the sample cell slowly. The sample cell is shown in Fig. 3(a). A natural gradient formed across the cell, with the bottom of the cell being warmed by heating from the fill tube heater used to keep it unblocked during crystal growth. Constant-pressure conditions were closely achieved by using the dead volume of the high-pressure gauge (above 30 cm^3) as a ballast. Crystal growth was monitored by watching the temperature of the bottom germanium thermometer. Figure 3(b) shows a typical growth curve.

Crystal-growth times varied over a wide range, as short as 45 min to as long as 11 h. The quality of the crystal does not seem to be strongly correlated with growth time. The exception is that when very fast growth occurs, the large temperature gradient which is necessary seems to segment the crystal. Specimen quality was checked two ways. The first was by transmission Laue photographs which also provided the orientation of the crystal. The second was by examining the initial Θ-Θ scans taken at various heights along the crystal. It was found that only completely single crystals yielded reliable data. A common growth fault was bicrystallinity, which was shown by each spot on a transmission Laue photograph becoming a closely spaced doublet.[33] This resulted in the rejection of a large number of crystals.

IV. DATA

A. X-ray data

Out of approximately 100 crystals grown, 21 passed the initial screening just described and were used for data scans. The crystals seemed to be very sensitive to temperature changes and care had to be exercised during data taking to avoid nonreproducible behavior of the lattice parameter. If repeated scans were taken at a constant temperature the lattice parameter reproducibility was about 50 ppm. Changing the temperature often resulted in the scatter of the data being increased. The source of this behavior was likely due to stresses induced by pressure gradients in the cell as the temperature was changed. As such it most frequently occurred near melting where $(\partial P/\partial T)_V$ is the greatest. Therefore, on later crystals the region near melting was avoided until late in the run.

The sensitivity of the crystals to temperature changes sometimes caused bicrystallinity to be revealed only after the first few temperature changes. This resulted in the re-

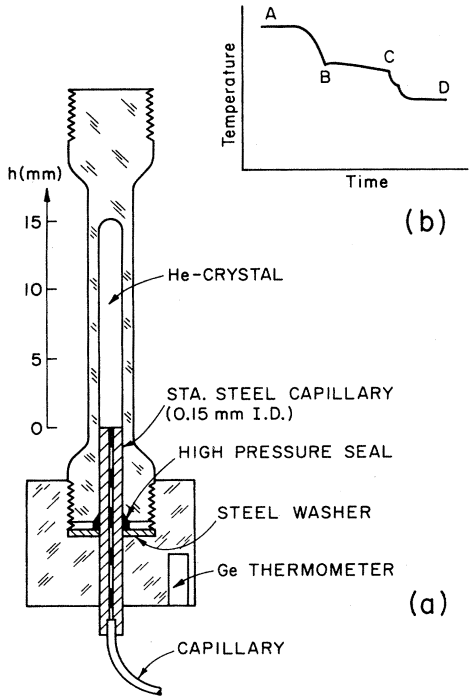

FIG. 3. (a) Plastic sample cell. Lucite was used for pressures below 8 MPa and Delrin was used for higher pressures. (b) A typical crystal-growth curve as recorded on a strip chart from the germanium thermometer. The various segments of the curve are interpreted as follows: A, start cooling top of cell; B, start of crystal growth at top of cell; C, finish of crystal growth; D, temperature equilibrium established as thermal gradients across the specimen decay away.

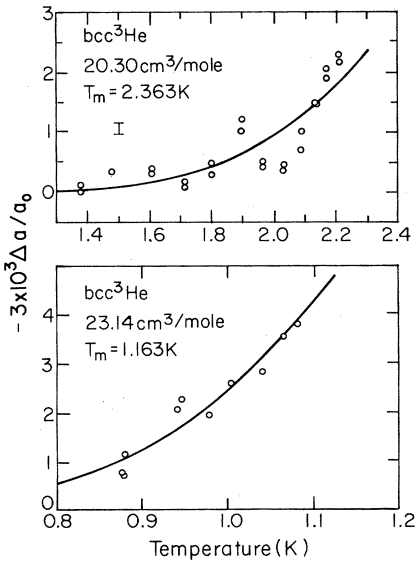

FIG. 4. Examples of data taken on bcc ^{3}He crystals grown at the molar volumes indicated. The error bar in the upper graph is the estimated precision of the diffractometer. The additional scatter of the data points seems to be intrinsic to the crystals under the conditions of the experiment (see Sec. IV A). T_m is the melting temperature and $-3\Delta a/a_0$ is the vacancy concentration. The solid lines are exponential least-squares fits and were used to set a_0 as well as to find the free energy f_v. The data for 20.30 cm^3/mole were taken on cooling, and those for 23.14 cm^3/mole were taken on warming.

TABLE II. Physical parameters of the crystals used for data, along with the f_v value found from a simple exponential fit. Stated errors for the f_v values of the bcc crystals are twice the standard deviations given by the fitting program. The error limits for the hcp crystal contain an additional factor due to a lack of knowledge about the temperature dependence of the c/a ratio [for a discussion of the application of the present x-ray technique to hexagonal crystals, see R. Feder and A. S. Nowick, Phys. Rev. B 5, 1238; 5, 1244 (1972). A $(10\bar{1}1)$ Bragg peak was measured here.], which was not measured in this experiment. The last column is a measure of the number of vacancies at melting. For the bcc crystals the vacancy concentration at melting averages very close to 5×10^{-3} ($f_v/T_m=5.3$).

Crystal	Pressure (MPa)	T_m (K)	Vol. (cm^3/mole)	Growth time (h)	f_v (K)	f_v/T_m
3	6.84	1.800	21.49	2	9.50±0.46	5.28
4	8.32–8.34	2.190	20.84	3	11.10±1	5.07
7	9.72–9.63	2.363	20.30		13.96±0.54	5.89
8 (hcp)	13.78–13.76	3.149	18.8	$1\frac{1}{2}$	$21.4\ ^{+1.2}_{-1.6}$	6.79
9	3.18	0.619	24.58	3	2.96±0.14	4.78
10	3.16	0.605	24.61	$5\frac{1}{2}$	3.20±0.22	5.28
11	3.16	0.605	24.61	11	3.40±0.24	5.62
12	3.48	0.779	24.20	4	4.25±0.10	5.32
20	2.98	0.435	24.86	$\frac{3}{4}$[a]	2.29±0.22	5.26
21	4.49	1.163	23.14	$2\frac{1}{4}$	6.02±0.24	5.17

[a]Grown by warming from below the minimum in the melting curve.

jection of several of the original 21 crystals. Also, a few other crystals were rejected because of dramatic changes in the Bragg-peak intensity and shape during the period of data collection. In the present apparatus, crystals grown near the molar volume 23 cm^3/mole (T_m about 1.16 K) seemed particularly unstable. Crystals 13 through 19 were unsuccessful attempts at taking data near this molar volume. Accordingly, ten crystals were finally selected for extensive data taking and analysis. The properties of these usable crystals are summarized in Table II. Some examples of the data obtained on the crystals are shown in Figs. 4 and 5. Other data are shown in Ref. 26. The solid lines on these figures are simple exponential fits which would describe the vacancy concentration if the free energy of formation, f_v, is constant. Such would be the case if the vacancies are localized and s_v is near zero, since for helium the correction term in Eq. (11) is small.

B. Possible corrections to x-ray data

Equation (2) gives the vacancy concentration only if the entire lattice parameter change is due to vacancies. For example, the formation of an interstitial causes a lattice parameter change opposite to that of a vacancy. Thus, the creation of vacancy-interstitial pairs leaves the lattice parameter unchanged. Calculations by Mullin[34] indicate that the formation of an interstitial, either isolated or in association with a vacancy, requires much more energy than the formation of a vacancy. Hetherington[1] also gives arguments suggesting that vacancies are the dominant thermal defects. We therefore assume that interstitial formation can be neglected.

Another possible contribution to Δa is the volume change caused by the formation of dislocations. In linear elastic theory creation of a dislocation has no volume change associated with it. Very near the dislocation, how-

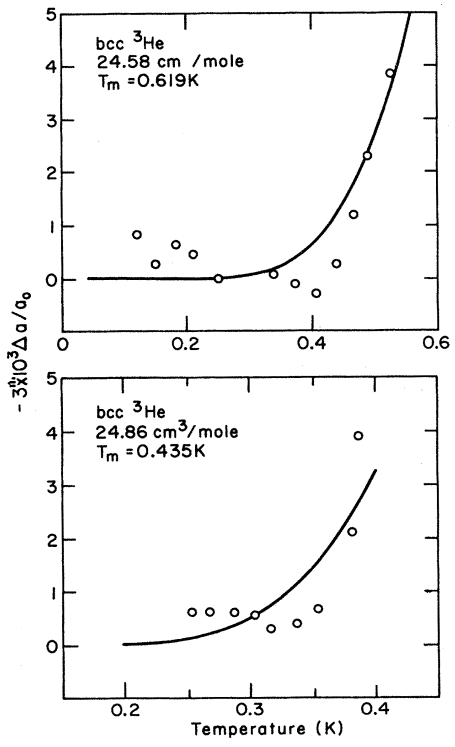

FIG. 5. Examples of data taken on large molar volume bcc ^{3}He crystals. T_m is the melting temperature and $-3\Delta a/a_0$ is the vacancy concentration. The lines are exponential least-squares fits and were used to set a_0 as well as to find f_v. The crystal for 24.86 cm^3/mole was grown by warming from below the minimum in the melting curve and the points were taken on warming.

ever, elastic theory breaks down and the possiblity of a volume change exists. Holder and Granato[35] have calculated the volume change due to dislocations for a large number of materials, and find that it is about an atomic volume per atomic length of dislocation. A volume change $\Delta V/V=10^{-4}$ would thus require about 10^{11} cm/cm^3 of dislocations. Ultrasonic attenuation measurements[36] give dislocation densities for ^{4}He in the range 10^6—10^9 cm/cm^3, and for ^{3}He, smaller.[12] Such densities would be undetectable by the current x-ray method.

Diffuse x-ray scattering can cause apparent shifts of the Bragg peak with changes in temperature. This occurs because some sources of diffuse scattering do not contribute symmetrically to the intensity on opposite sides of the Bragg peak. Diffuse scattering arises from factors which disturb the periodicity of the lattice. These include the motion of the atoms about their equilibrium positions due to thermal vibrations or zero-point motion, and the distortion of the lattice due to defects.

Thermal (lattice) diffuse scattering is approximately proportional to Q^2 where Q is the scattering vector.[37] Therefore, the apparent center of the Bragg peak is shifted to higher Q values. If the observed peak is roughly Gaussian in shape, to get an estimate of the magnitude of the shift we write the peak intensity as

$$I=Q^2\exp[-b^2/(Q-G)^2]\,. \tag{20}$$

If b^2 is fit to give the observed peak width and the entire peak is assumed to be from diffuse scattering, the Bragg peak is shifted by an amount $-3\,\Delta a/a=10^{-4}$ from the true Bragg-peak location G. Since the measured peak certainly has some Bragg component, the actual shifts are smaller. Because of the large zero-point motion in helium, thermal vibrations constitute only a small portion of the atomic motion. Thus, diffuse scattering due to atomic vibrations is likely to be largely temperature independent, resulting in a constant shift of the apparent lattice parameter.

The theory of diffuse scattering due to defects is reviewed by Dederichs.[38] Close to the Bragg peak this scattering images primarily the long-range strain field of the defect, and can be broken into two parts. The first is symmetric or Huang scattering and has no effect on the peak location. The second part is the antisymmetric scattering which varies as Q^{-1}. The sign of the asymmetry is such that it shifts the Bragg peak to smaller angles, partially canceling the shift due to the vacancies.

Since detailed calculations are difficult, we compare helium with a well-characterized substance such as aluminum.[39] For aluminum at room temperature it is found that the magnitude of the diffuse scattering from an interstitial concentration of 5×10^{-4} is somewhat smaller than thermal diffuse scattering for low-order Bragg reflections. Diffuse scattering from interstitials is typically 10 times stronger than that from vacancies. This means the above interstitial concentration for aluminum is roughly equivalent to the vacancy concentration in helium at melting. However, for helium the lattice diffuse scattering is a much larger part of the observed Bragg reflection because of zero-point motion. We therefore believe that the diffuse scattering from the vacancies in helium should comprise only a small fraction of the observed peak, and have a negligible effect on the Bragg-peak location.

To summarize, it appears that all these possible corrections to Δa are sufficiently small to be neglected. We therefore assume that the lattice parameter changes represent changes in vacancy concentration.

V. DATA ANALYSIS

A. Comparison to other results

Figure 6 is a comparison for the bcc phase of the vacancy-formation free energies listed in Table II with previous measurements. The NMR results[9–11] are actually diffusion activation energies (see Sec. II B). The ultrasonic points[12] were obtained by following the recovery, at a succession of increasing annealing temperatures, of attenuation introduced in specimens near 100 mK by high-amplitude 3-MHz pulses; the resulting activation energies apply to diffusion.

In the bcc phase all the data appear in good agreement within their respective experimental uncertainties. The x-ray measurements of Balzer and Simmons[25] are systematically slightly low. A possible explanation lies in the fact that they did not reach sufficiently low temperatures to accurately determine a_0. A similar situation occurred for crystal 4 which is the point at 20.8 cm^3/mole. Without an accurate value of a_0 it is easy to overestimate the number of vacancies, and the point for crystal 4 is closer to the results of Balzer and Simmons than others of the present work.

If the vacancy band due to possible vacancy nonlocalization is assumed to be narrow the classical localized vacancy formulas can still be used. The NMR data then provide the energy $e_{\rm NMR}=e_v+E_b$. Because the NMR results were analyzed assuming a constant $e_{\rm NMR}$, these values are slightly incorrect since according to Eq. (10) e_v should have a slight temperature dependence. However, the value of $e_{\rm NMR}$ does not depend on the choice of s_v, because s_v is absorbed into a preexponential factor and does

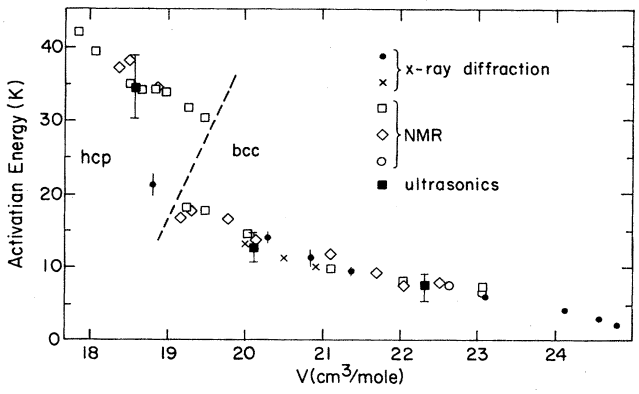

FIG. 6. Comparison of vacancy formation (activation) energies as determined by various techniques. The NMR data of Reich (Ref. 9), Sullivan and co-workers (Ref. 10), and Bernier and Guerrier (○, Ref. 11) are diffusion activation energies. The points of Beamish and Franck (Ref. 12) are inferred indirectly from ultrasonic measurements, and the points of Balzer and Simmons (×, Ref. 25) and the present work (○) are free energies from direct x-ray measurements.

not affect the value found for e_v.

From the present x-ray measurements only the free energy of formation f_v can be determined. Thus, the value of e_v depends on the choice of s_v. The apparent agreement of the NMR and ultrasonic results on the one hand and the present x-ray results on the other, in Fig. 6, leads to two possible conclusions. (1) The vacancies tunnel, which means $e_{\rm NMR}=e_v\simeq f_v$. This would imply $s_v\simeq 0$. (2) The vacancies are not tunneling, but jump over a small barrier in which case $e_{\rm NMR}=e_v+E_b\simeq f_v$. Then from Eq. (4) and the measured vacancy concentration it must be true that $S_v/k\simeq E_b/T_m$, where T_m is the melting temperature. T_m is used since the present x-ray measurements only provide the vacancy concentration accurately near melting. Since it is unlikely that E_b is volume independent, it seems unlikely that the second conclusion would hold for all molar volumes. We therefore conclude that the tunneling hypothesis is the most probable, although more information about s_v in the bcc phase would be desirable.

For the hcp phase at 18.8 cm^3 the x-ray formation energy in Table II is much lower than the NMR diffusion activation energy at that molar volume. This is strong evidence that diffusion in the hcp phase proceeds classically (i.e., by a thermally activated process), and that any tunneling mechanism makes at most a small contribution to the overall diffusion constant. From the difference between the x-ray and NMR values the barrier to an atomic jump into a vacant site can be estimated. Assuming that the vacancy entropy of formation is near zero the barrier is about 12 K. These conclusions verify the speculations of Sullivan and co-workers.[10] Their data seemed to be inconsistent with a tunneling hypothesis in the hcp phase and they estimated a barrier height of 13 K.

Since classical diffusion appears to be occurring in the hcp phase, the value of $\tau_0(=2\pi/\omega_0)$ from Ref. 10 can be used to calculate the diffusion activation entropy. Classical transition-rate theory gives[40]

$$S_d/k=\ln(D_0/\gamma\nu a^2)\,, \tag{21}$$

where γ is a geometrical constant (equal to 1 for an hcp lattice), a is the nearest-neighbor distance, ν is the vibrational frequency of the atom, and D is related to τ_0 by[30]

$$D=\frac{a^2}{6\tau_0}\,. \tag{22}$$

Combining Eqs. (21) and (22) and using the Debye frequency for ν, we find $s_d=-2.9k$. The actual value of s_d probably should not be taken too seriously since $T/\Theta\lesssim 0.1$. This means that the average vibrational frequency of the atom is less than the Debye frequency. It would appear, however, that in the hcp phase the activation entropy of diffusion is somewhat negative.

B. Vacancy free volume of formation

The free volume of formation can be inferred in several different ways. (1) One source of information about the vacancy volume is from NMR experiments. The pressure dependence of the relaxation times T_1 or T_2 provides the free volume of diffusion for the vacancies. The volume of diffusion is an upper limit on the vacancy volume, since $v_d=v_p+v_m$ where v_m is the free volume of migration. (2) From the present measured values for the number of vacancies, the free volume of formation, v_p, can be calculated from the volume dependence of f_v as determined by the x-ray measurements. This requires using Eq. (12) to convert $(\partial f_v/\partial V)_T$ into free volumes. We consider these in turn.

The only previous volume determination is of the free volume of diffusion, v_d. Goodkind and Fairbank[41] measured the pressure dependence of T_1 and T_2 and found a value $v_d\approx 7.3$ cm^3/mole independent of pressure over a range from 5.5 to 11 MPa. Later NMR results were not analyzed to obtain v_d. Therefore, seeking more information about v_d, we analyzed the T_1 measurements of Sullivan and co-workers.[10] As shown in Fig. 7, these results differ from that of Goodkind and Fairbank. Possibly this is related to the fact that Sullivan and co-workers[10] used a constant-pressure crystal-growing technique which should produce nearly single crystals (for which T_1 shows some anisotropy), while the analysis is appropriate for polycrystalline samples. This is further complicated by the fact that data from four different crystals were used to calculate v_d values from the data of Sullivan and co-workers. On the other hand, the technique of Goodkind and Fairbank should produce polycrystals, and the same specimen was used throughout a given set of T_1 or T_2 measurements. This avoids problems associated with any sample dependence of the relaxation times.

Second, the relations in Table I provide two ways of inferring values of v_p. The vacancy contributions to the thermal-expansion coefficient and the isothermal compressibility both depend on the vacancy volume. The difficulty in applying these formulas lies in isolating the va-

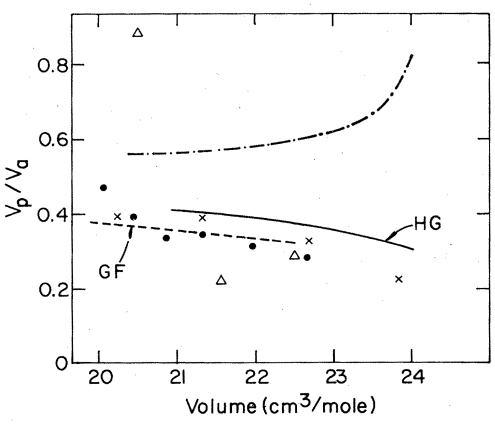

FIG. 7. Vacancy free volume of formation as determined by various methods. (×) Comparison of present x-ray measurements with thermal-expansion measurements (Ref. 42). (○) Comparison of present x-ray measurements and compressibility measurements (Ref. 42). (△) Present analysis of the NMR T_1 data in Ref. 10. (GF) Value of v_d/v_a found by Goodkind and Fairbank (Ref. 41). (HG) Calculation based on the theory of Holder and Granato (Ref. 35). The dashed-dotted curve is from an analysis of x-ray data assuming localized vacancies and $s_v=0$.

cancy contribution.

Straty and Adam[42] have made measurements of the compressibility away from melting. Since the temperature dependence of the compressibility is small, these early measurements are not of high accuracy. Therefore, instead of attempting to subtract the lattice contribution, we obtain an upper limit on v_p by setting all of the measured change equal to $\beta_T - \beta_T^0$. In performing this calculation the derivative $(\partial v_p/\partial P)_T$ is ignored since it makes only a minor contribution to $\beta_T - \beta_T^0$. That this is true can be seen from the theory of Holder and Granato[35] and it is verified by the final results for v_p. These results are shown in Fig. 7 as the solid circles.

The lattice contribution to the volume thermal expansion is related to the lattice-heat capacity by

$$\alpha^0 = \frac{\gamma C_V^0 \beta_T}{V} , \tag{23}$$

where γ is the lattice Gruneisen constant. The present calculation uses the low-temperature thermal expansion to determine γC_V^0. Since the vacancy concentration decreases exponentially, at sufficiently low temperatures the thermal expansion is determined largely by the lattice. In the Debye approximation

$$C_V = 234R\left[\frac{T}{\Theta}\right]^3 . \tag{24}$$

Therefore, for a given γ, Θ_0 is calculated at low temperatures using Eqs. (23) and (24). The lattice contribution α_0 can then be subtracted at temperatures near melting where the vacancies dominate the measured α. The thermal-expansion data of Straty and Adams[42] were used. v_p/v_a is calculated using the equation in Table I and the measured number of vacancies. Again the small derivative term is ignored. An expected small-temperature dependence of Θ was estimated using the "universal" curve of $\Theta(T)/\Theta_0$ calculated for bcc ^{3}He by deWette and coworkers.[43] The results for v_p/v_a near melting using this procedure are insensitive to choice of γ in the range 2.2 to 2.8 and are plotted in Fig. 7.

Also shown in Fig. 7 is the calculated volume dependence of v_p/v_a using the theory of Holder and Granato.[35] Their theory gives for the volume of a defect

$$\frac{v_p}{g_p} = \frac{G'}{G} - \frac{1}{B_T} , \tag{25}$$

where G is the shear elastic constant, G' is the pressure derivative of G, and B_T is the bulk modulus. To calculate the curve in Fig. 7, G and G' were calculated from measured elastic constants[40] and g_p was taken to be the same as the measured values of activation energy. Since the elastic constants are only known at essentially two pressures (the pressures corresponding to a molar volume of 21.66 and molar volumes near 24 cm^3/mole), a linear pressure dependence was assumed. The exact shape of the curve is, therefore, uncertain, although the magnitude and general trend should be correct.

Third, the x-ray data can also be used alone to estimate v_p. In principle, a logarithmic derivative of the vacancy concentration with respect to pressure yields v_p. However, because of the limited sensitivity of the present x-ray technique the vacancy concentration can be measured only in a narrow temperature range near melting. Thus, because of the relatively large change of T_m with pressure, a direct comparison of vacancy concentrations at a given temperature cannot be made for different crystals unless they are grown at very similar pressures. Some functional form has to be assumed in order to smooth out the scatter of the x-ray data and to calculate the vacancy concentration at temperatures away from melting. The exponential fits shown in the data plots and given in Table II are appropriate for the localized vacancy case with $s_v \simeq 0$. Then in that case f_v is nearly temperature independent, and its value found near melting can be used at low temperatures. The use of this assumption and Eqs. (7) and (12) to convert the volume dependence of f_v into a vacancy volume, leads to the dashed-dotted curve in Fig. 7.

Considering the uncertainty involved in the various determinations of v_p, the agreement in Fig. 7 is good. The "localized vacancy" curve resulting from the last analysis is the exception; it has a different magnitude and volume dependence. Because the other determinations involve comparisons of directly measured numbers to obtain v_p/v_a (or v_d/v_a), they are relatively insensitive to the microscopic nature of the vacancies and can be taken with some confidence. However, the "localized" values depend on the assumed temperature independence of f_v, which in turn depends on the microscopic nature of the vacancy (nonlocalized or localized?). The disagreement of the localized curve thus suggests the possibility of nonlocalized vacancies.

C. Vacancy heat capacity

From Eqs. (10) and (16), the heat capacity of a localized vacancy system can be calculated now that the number of vacancies is known. The results near 21.5 cm^3/mole (Ref. 44) are shown in Fig. 8 for this assumption [$s_v \simeq 0$ and the only temperature dependence of e_v is from Eq. (10)]. It is seen that the inferred heat capacity of the defect-free crys-

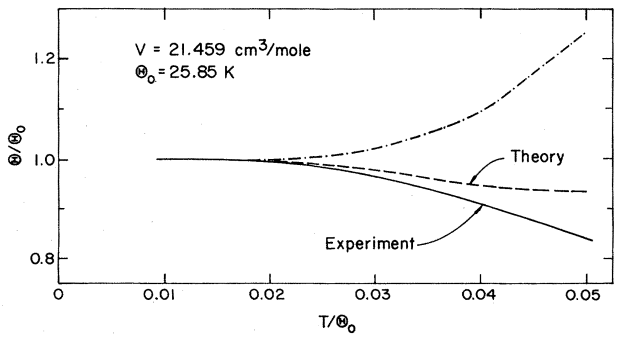

FIG. 8. Equivalent Debye characteristic temperatures for the heat capacity. The solid curve represents data of Greywall (Ref. 44) at $V = 21.459$ cm^3/mole. The dashed curve is a calculation for the defect-free crystal (Ref. 43), which is to be compared to the dashed-dotted curve obtained by subtracting a localized vacancy contribution with $f_v = 9.5$ K from the experimental heat capacity (see text Sec. V C).

tal (dashed-dotted curve) is much smaller than that expected from theory.[43] In fact, such an estimate for molar volumes greater than 24 cm^3/mole yields an inferred heat capacity of the vacancies larger than the total measured heat capacity. Again this result suggests the possibility of nonlocalized vacancies, such that e_v is less than f_v.

However, two other possibilities also come to mind. One is the possibility that large numbers of vacancies are bound into divacancies or larger vacancy clusters, and the other is the possiblity of a nonzero formation entropy. We therefore considered divacancies using Eq. (19) and several assumptions for the divacancy binding energy. Implicit in these estimates was the constraint that the x-ray measurements measure the total number of vacant sites $n=n_1+2n_2$ where n_1 and n_2 are the numbers of monovacancies and divacancies, respectively. It was found that even for the extreme assumption $b_2=f_v/2$, the heat capacity of the vacancy-plus-divacancy system at melting is comparable to the heat capacity of the corresponding monovacancy system. Thus, it seems that the heat capacity and x-ray results cannot be reconciled by a classical treatment of vacancy interactions.

A nonzero entropy of formation can also change the estimate of vacancy heat capacity. Since f_v is fixed by the x-ray measurements, e_v depends on the value assumed for s_v [see Eq. (4)]. We see that in order to reduce e_v, s_v must be negative. From Sec. V A a negative s_v seems unlikely but is not ruled out by the data. The entropy of formation is discussed by Hetherington[45] and Widom and coworkers[46] who find that vacancy nonlocalization can result in an apparent negative entropy of formation if the results are analyzed using localized vacancy assumptions. Thus an apparent negative entropy of formation again seems to lead to the possibility of vacancy nonlocalization. Clearly, more definite conclusions await more detailed knowledge of the vacancy-formation entropy.

Greywall,[44] Hetherington,[45,47] and Widom and coworkers[46] have all used Greywall's specific-heat data to infer a free energy of vacancy formation. Each of these analyses claims independence of a specific microscopic model for ^{3}He vacancies. However, their inferences differ as to whether the specific-heat data and the directly measured vacancy concentrations are compatible. Recent NMR work at molar volumes above 23 cm^2/mole has been interpreted[48] in terms of even larger vacancy concentrations than those given by the present x-ray measurements.

VI. CONCLUSIONS

We have shown that thermal vacancy concentrations can be measured directly by x-ray diffraction over a wide range of molar volumes in ^{3}He, including large molar volumes for which specimens have both upper and lower melting temperatures. The data do show some scatter, beyond that intrinsic to the x-ray method, so they have mostly been analyzed using the simplest assumptions. The deduced vacancy-formation energies in bcc ^{3}He essentially agree with diffusion energies obtained from NMR and ultrasonic experiments, while they are significantly less than diffusion energies in hcp ^{3}He. These comparisons suggest that vacancies tunnel between lattice sites in the bcc phase and move by a thermally activated process in the hcp phase. Verification of this result awaits more knowledge of the vacancy entropy of formation.

From the x-ray values of vacancy concentration one can obtain, by comparisons using other thermal-expansion, compressibility, elastic constant, and NMR measurements, (a) values of the bcc ^{3}He vacancy free volume of formation and its volume dependence, and (b) note that within the respective uncertainties of the estimates there is essentially zero free volume of migration (or tunneling). The formation volume can also be estimated from the volume dependence of the free energy of formation. Such an analysis for the bcc phase suggests that a localized vacancy picture is inadequate. A similar conclusion is reached from a consideration of the apparent vacancy heat capacity. Again, however, the need for a more detailed knowledge of the vacancy-formation entropy and/or nonlocalization is indicated. In addition, the large (about 0.5%) vacancy concentrations in bcc ^{3}He near melting suggest that interactions between vacancies are probably important.

ACKNOWLEDGMENT

This research was supported by the Division of Materials Sciences, U. S. Department of Energy, under Contract No. DE-AC02-76ER01198.

*Present address: Brookhaven National Laboratory, Upton, NY 11973.

†Present address: Battelle Pacific Northwest Laboratories, Richland, WA 99352.

[1]J. H. Hetherington, Phys. Rev. **176**, 231 (1968).

[2]A. F. Andreev and I. M. Lifshitz, Zh. Eksp. Teor. Fiz. **56**, 2057 (1969) [Sov. Phys.—JETP **29**, 1107 (1969)]; A. F. Andreev, in *Progress in Low Temperature Physics,* edited by D. F. Brewer (North-Holland, Amsterdam, 1982), Vol VIII, Chap. 2.

[3]R. A. Guyer, J. Low. Temp. Phys. **8**, 427 (1972).

[4]A. Landesman, Ann. Phys. (N.Y.) **9**, 69 (1975).

[5]H. Bolterauer and P. Gilleson, J. Low Temp. Phys. **26**, 193 (1977).

[6]M. Héritier and P. Lederer, J. Phys. (Paris) Lett. **38**, L209 (1977); J. Phys. (Paris) Colloq. **39**, C6-130 (1978).

[7]Yu. Kagan and L. A. Maksimov, Phys. Lett. A **95**, 242 (1983).

[8]R. A. Guyer, R. C. Richardson, and L. I. Zane, Rev. Mod. Phys. **43**, 532 (1971).

[9]H. A. Reich, Phys. Rev. **129**, 630 (1963).

[10]N. Sullivan, G. Deville, and A. Landesman, Phys. Rev. B **11**, 1858 (1975).

[11]M. E. R. Bernier and G. Guerrier, Physica **121B**, 202 (1983); also, in *Quantum Fluids and Solids—1983 (Sanibel Island, Florida),* Proceedings of the Symposium on Quantum Fluids and Solids, edited by E. D. Adams and G. G. Ihas (AIP, New York, 1983), p. 69.

[12]J. R. Beamish and J. P. Franck, Phys. Rev. Lett. **47**, 1736

(1981); Phys. Rev. B **28**, 1419 (1983).
[13]I. Iwasa and H. Suzuki, J. Phys. (Paris) Colloq. **42**, C6-896 (1981); J. Phys. Soc. Jpn. **51**, 2116 (1982).
[14]E. C. Heltemes and C. A. Swenson, Phys. Rev. Lett. **7**, 363 (1961).
[15]D. O. Edwards, A. S. McWilliams, and J. G. Daunt, Phys. Lett. **1**, 218 (1962).
[16]H. H. Sample and C. A. Swenson, Phys. Rev. **158**, 188 (1967).
[17]D. S. Greywall, Phys. Rev. B **15**, 2604 (1977); **16**, 5129(E) (1977).
[18]R. Feder and A. S. Nowick, Phys. Rev. **109**, 1959 (1958).
[19]R. O. Simmons and R. W. Balluffi, J. Appl. Phys. **30**, 1249 (1959); Phys. Rev. **117**, 52 (1960).
[20]R. O. Simmons, in *Rendiconti della Scuola International de Fisica "E. Fermi"—XVIII Corso,* edited by D. S. Billington (Academic, New York, 1966), p. 568.
[21]D. L. Losee and R. O. Simmons, Phys. Rev. **172**, 934 (1968).
[22]W. E. Schoknecht and R. O. Simmons (unpublished).
[23]L. A. Schwalbe, Phys. Rev. B **14**, 1722 (1976).
[24]For other variants, see A. T. Macrander, Phys. Rev. B **21**, 2549 (1980); P. R. Granfors, A. T. Macrander, and R. O. Simmons, *ibid.* **24**, 4753 (1981).
[25]R. Balzer and R. O. Simmons, in *Low Temperature Physics LT13,* edited by D. K. Timmerhaus, W. J. O'Sullivan and E. F. Hammel (Plenum, New York, 1974), Vol. 2, p. 115.
[26]A preliminary account has appeared: S. M. Heald, D. R. Baer, and R. O. Simmons, Solid State Commun. **47**, 807 (1983).
[27]C. P. Flynn, *Point Defects and Diffusion* (Clarendon, Oxford, 1972), Chap. 2; A. W. Chadwick and H. R. Glyde, in *Rare Gas Solids,* edited by M. L. Klein and J. A. Venables (Academic, New York, 1977), Vol. II, p. 1151.
[28]W. E. Schoknecht and R. O. Simmons (unpublished).
[29]W. E. Schoknecht and R. O. Simmons, in *Thermal Expansion—1971 (Corning),* Proceedings of the 1971 Thermal Expansion Symposium, edited by M. Graham and H. E. Hagy (AIP, New York, 1971), p. 169.
[30]A. Landesman, J. Low Temp. Phys. **17**, 365 (1974).
[31]S. M. Heald and R. O. Simmons, Rev. Sci. Instrum. **48**, 316 (1977).
[32]R. O. Simmons, Trans. Am. Cryst. Soc. **17**, 17 (1981).
[33]B. A. Fraass, S. M. Heald, and R. O. Simmons, J. Cryst. Growth **42**, 370 (1977).
[34]W. J. Mullin, Phys. Rev. A **4**, 1247 (1971).
[35]J. Holder and A. V. Granato, Phys. Rev. **182**, 729 (1969).
[36]R. Wanner, I. Iwasa, and S. Wales, Solid State Commun. **18**, 853 (1976); Y. Hiki and F. Tsurouka, Phys. Lett. **56A**, 484 (1976).
[37]B. Donovan and J. F. Angress, *Lattice Vibrations* (Chapman and Hall, London, 1971), p. 128.
[38]P. H. Dederichs, J. Phys. F **3**, 471 (1973).
[39]H. Peisl, J. Appl. Cryst. **8**, 143 (1975).
[40]G. J. Dienes, Phys. Rev. **89**, 185 (1953).
[41]J. M. Goodkind and W. H. Fairbank, in *Helium Three,* edited by J. G. Daunt (Ohio State University Press, Columbus, 1960), p. 52
[42]G. C. Straty and E. D. Adams, Phys. Rev. **169**, 232 (1968).
[43]F. W. deWette, L. H. Nosanow, and N. R. Werthhamer, Phys. Rev. **162**, 824 (1967); F. W. deWette and N. R. Werthhamer, *ibid.* **184**, 209 (1969).
[44]D. S. Greywall, Phys. Rev. B **15**, 2604 (1976); **16**, 5129(E) (1977).
[45]J. H. Hetherington, Fiz. Nizkikh Temp. **1**, 613 (1975) [Sov. J. Low Temp. Phys. **1**, 295 (1975)].
[46]A. Widom, J. B. Sokoloff, and J. E. Sacco, Phys. Rev. B **18**, 3293 (1978).
[47]J. H. Hetherington, J. Low Temp. Phys. **32**, 173 (1978).
[48]M. Chapellier, M. Bassou, M. Devoret, J. M. Delreiu, and N. S. Sullivan, in *Quantum Fluids and Solids—1983,* edited by E. D. Adams and G. G. Ihas (AIP, New York, 1983), p. 81.